Int J Ind Chem (2017) 8:433–445
https://doi.org/10.1007/s40090-017-0132-1

RESEARCH

Effect of γ-Fe_2O_3 nanoparticles on rheological and volumetric properties of solutions containing polyethylene glycol

Somayyeh Navidbakhsh[1] · **Roghayeh Majdan-Cegincara**[1]

Received: 8 December 2016 / Accepted: 1 November 2017 / Published online: 9 November 2017

Abstract The effect of γ-Fe_2O_3 nanoparticles on the rheological and volumetric properties of polyethylene glycol with molar mass of 400 (g mol^{-1}), PEG400, and the dilute solutions of PEG400-PEG2000 and PEG400-PEG6000 was investigated. PEGs with molar masses of 2000 and 6000 (g mol^{-1}) were dissolved in PEG400 to prepare the homogeneous solutions. Rheological properties and the density values for these solutions were measured. Nanoparticles of γ-Fe_2O_3 were added to these solutions and dispersed by an ultrasonic bath for making the homogeneous nanofluids. The UV–Vis spectroscopy, zeta potential and dynamic light scattering have been used to specify the stability and particle size distribution of colloidal solutions studied. Fluid flow and suspense structure of γ-Fe_2O_3 nanoparticles in the base fluids of PEG400, PEG400-PEG2000 and PEG400-PEG6000 were studied by measuring the magnetorheological properties at $T = 298.15$ K. Bingham plastic, Herschel–Bulkley, and Carreau–Yasuda models have been applied for modeling the magnetorheological properties of nanofluids. Interparticle interactions that occurred in the investigated nanofluids can be determined by calculating the excess molar volume values. This requires to measure the density data for γ-Fe_2O_3-PEG400, γ-Fe_2O_3-PEG400-PEG2000 and γ-Fe_2O_3-PEG400-PEG6000 systems at $T = (298.15, 308.15$ and $318.15)$ K. The excess molar volumes were calculated from these data and fitted with Ott et al. and Singh et al. equations.

Keywords Nanofluids · γ-Fe_2O_3 nanoparticles · Polyethylene glycol · Magnetorheological property · Density

Introduction

The dilute colloidal fluids of nanosized particles in the heat transfer liquids are a matter of interest due to their single thermal behavior. Stable colloidal solutions that consist of magnetite, hematite and maghemite are called ferrofluids [1]. Ferrofluids have a great potential for development in the medical applications, mechanical engineering, electronic packing aerospace, etc. [1–4]. The low toxicity and water-soluble qualities of some polymers such as poly(ethylene glycol), PEG make them suitable for industrial applications. PEG and its derivatives are applied as surfactants, excipients in some drugs, lubricants, heat transfer fluid in electronic apparatus, gene therapy vectors, etc. [5]. Rheological properties are used to describe the flow behavior of fluids and also deformation of structures made in fluids. Rheological measurements also give the useful information for designing the colloidal solutions in the food industry, paint industry and heat transfer applications [6]. Because of large application field of ferrofluids, colloidal solutions containing Fe_2O_3 nanoparticles and polymers are topic of interest for some authors in the recent years. For example, the molar heat capacity for water-based α-Fe_2O_3 nanofluid prepared over a simple biomolecule-assisted hydrothermal method was measured by a high-precision automatic

Roghayeh Majdan-Cegincara or Roghayeh Majdan-Saghinsara.

Electronic supplementary material The online version of this article (https://doi.org/10.1007/s40090-017-0132-1) contains supplementary material, which is available to authorized users.

✉ Roghayeh Majdan-Cegincara
majdan@iaut.ac.ir; majdan944@gmail.com

[1] Department of Chemistry, Tabriz Branch, Islamic Azad University, Tabriz, Iran

adiabatic calorimeter at $T = (290–335)$ K by Wei et al. [7]. Guo et al. [8] have used a two-step method for preparation of magnetic nanofluids containing γ-Fe_2O_3 nanoparticles, ethylene glycol and water. Thermal transport properties for these nanofluids were also investigated by Guo et al. [8]. Colla et al. [9] measured the viscosity and thermal conductivity of water-based Fe_2O_3 nanofluid. Influence of the several surfactants in the colloidal stability, particle size distribution and thermal conductivity of water-based α-Fe_2O_3 nanofluids have been investigated by Gayadhthri et al. [10]. The structural changes of the oil-based ferrofluids were investigated under external magnetic fields by Rajnak et al. [11]. The magnetoviscous effect in the oil-based ferrofluids containing superparamagnetic oxide (Fe, Ni) in the presence of magnetic field was investigated by Katiyar et al. [12]. Felicia et al. [13] reviewed the recent advances in magnetorheological properties of ferrofluids. Rheology of a very dilute magnetic suspension with micro-structures of nanoparticles in mineral oil has been studied by Cunha et al. [14]. The stability and rheological properties of TiO_2 nanofluids containing PEG and also thermal conductivity of nanofluids containing carbon-coated metal nanoparticles and PEG were investigated previously [15, 16]. Rheological, magnetorheological and volumetric properties of nanofluids containing Fe_3O_4 nanoparticles and PEG have been investigated in our previous work [17].

In the present work, we prepared the homogeneous solutions of polyethylene glycols, PEGs, with molar masses of 2000 and 6000 (g mol^{-1}) in PEG with molar mass of 400 (g mol^{-1}). Rheological properties and density values for these solutions have been measured at different temperatures. Nanoparticles of γ-Fe_2O_3 were added to these solutions and dispersed by an ultrasonic bath for making the homogeneous nanofluids. The Ultraviolet–visible (UV–Vis) spectroscopy, zeta potential and dynamic light scattering have been used to specify the stability and particle size distribution of colloidal solutions studied. Rheological behaviors of γ-Fe_2O_3 nanoparticles dispersed in PEGs have been investigated in volumetric γ-Fe_2O_3 concentrations of $\varphi_1 = 1.5$ and 5% and shear rates ($\gamma = 0.01–1000$ s^{-1}) at different magnetic fields and 298.15 K. Bingham plastic

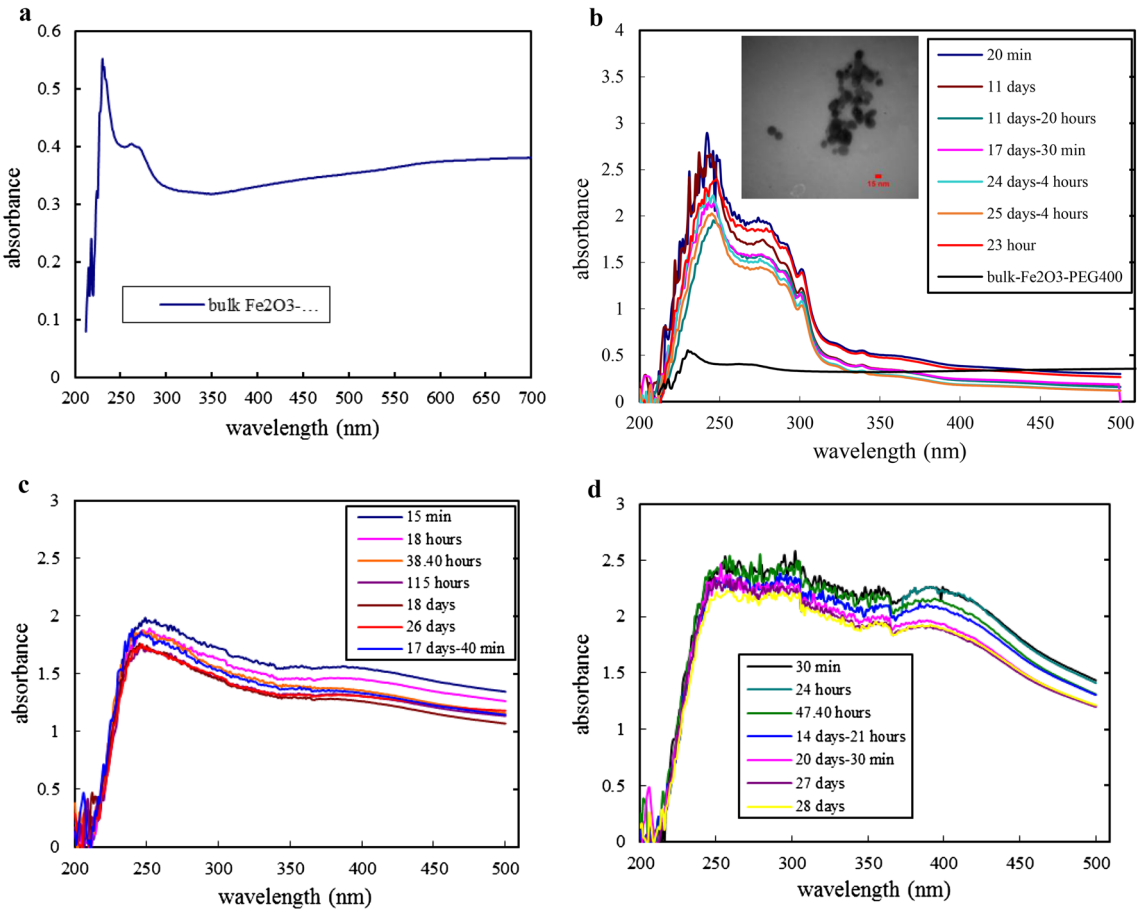

Fig. 1 UV–Vis absorption spectra for nanofluids: **a** bulk Fe_2O_3 in PEG400 at Fe_2O_3 mole fraction of 0.0004. **b** γ-Fe_2O_3 in PEG400 at γ-Fe_2O_3 mole fraction of 0.0008 and bulk Fe_2O_3 in PEG at Fe_2O_3 mole fraction of 0.0004 and TEM image of γ-Fe_2O_3 nanoparticle taken by producer. **c** γ-Fe_2O_3 in PEG400-PEG2000 at γ-Fe_2O_3 mole fraction of 0.0006. **d**: γ-Fe_2O_3 in PEG400-PEG6000 at γ-Fe_2O_3 mole fraction of 0.0009

[18], Herschel–Bulkley [18] and Carreau–Yasuda [19] models have been applied for modeling the magnetorheological properties of nanofluids. Density values of γ-Fe_2O_3-PEG400, γ-Fe_2O_3-PEG400-PEG2000 and γ-Fe_2O_3-PEG400-PEG6000 nanofluids have also been measured at $T = (298.15, 308.15$ and $318.15)$ K. The excess molar volumes were calculated from the density data for highlighting the interparticle interactions that occurred in nanofluids. Ott et al. [20] and Singh et al. [21] equations were used for fitting the excess molar volume values.

Experimental section

Materials

In this work, we used the bulk Fe_2O_3 with minimum mass fraction purity of 0.99 (Merck). γ-Fe_2O_3 nanoparticles with a moderate diameter of 20 nm and minimum mass fraction purity 0.995 were purchased from Nanostructured & Amorphous Materials, Inc. USA. γ-Fe_2O_3 nanoparticles were preserved under vacuum for 2 h to remove the water from surface of the particles, then kept in desiccators under argon atmosphere. PEG with molar masses of 400, 2000 and 6000 (g mol^{-1}) were also purchased from Merck and applied without any purification.

Preparation of nanofluids

PEGs with molar masses of 400 and 2000 (g mol^{-1}) with ratio of 275:1 were mixed at 328.15 K to make the homogeneous solution; then this solution got cold and γ-Fe_2O_3 nanoparticles were dispersed in the solution by applying the ultrasonic bath (Ultrasonic bath, Grant, Grant instruments (Cambridge) Ltd, England) for 4 h. The γ-Fe_2O_3-PEG400-PEG6000 nanofluid was also prepared same as γ-Fe_2O_3-PEG400-PEG2000 colloidal solution. The γ-Fe_2O_3 nanoparticles were also dispersed in PEG400 by using an ultrasonic bath (Ultrasonic bath, Grant, Grant instruments (Cambridge) Ltd, England) for 4 h to make the homogeneous suspension.

Apparatus

We used the analytical balance (Sartorius BP analytical balances Model BP301S) with an uncertainty of 0.1 mg for preparing the nanofluids of γ-Fe_2O_3-PEG400, γ-Fe_2O_3-PEG400-PEG2000 and γ-Fe_2O_3-PEG400-PEG6000. The UV–Vis spectra were recorded with spectrophotometer (Shimadzu UV-1700-Pharma). The particle size distribution of γ-Fe_2O_3 nanoparticles dispersed in PEG and zeta potential values of nanofluids were measured by the dynamic light scattering (DLS, Malvern, Nano ZS, ZEN

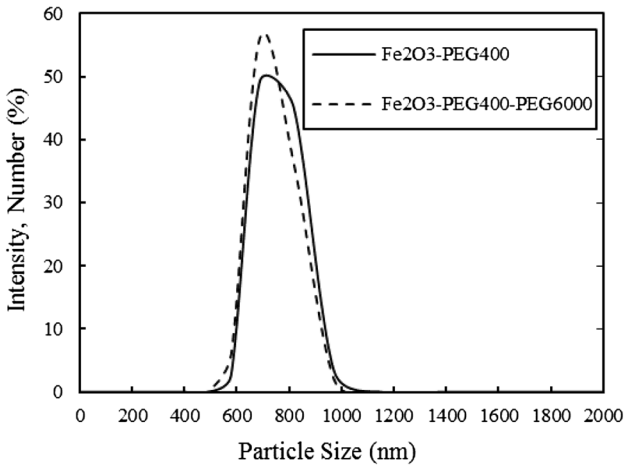

Fig. 2 Particle size distribution for investigated nanofluids

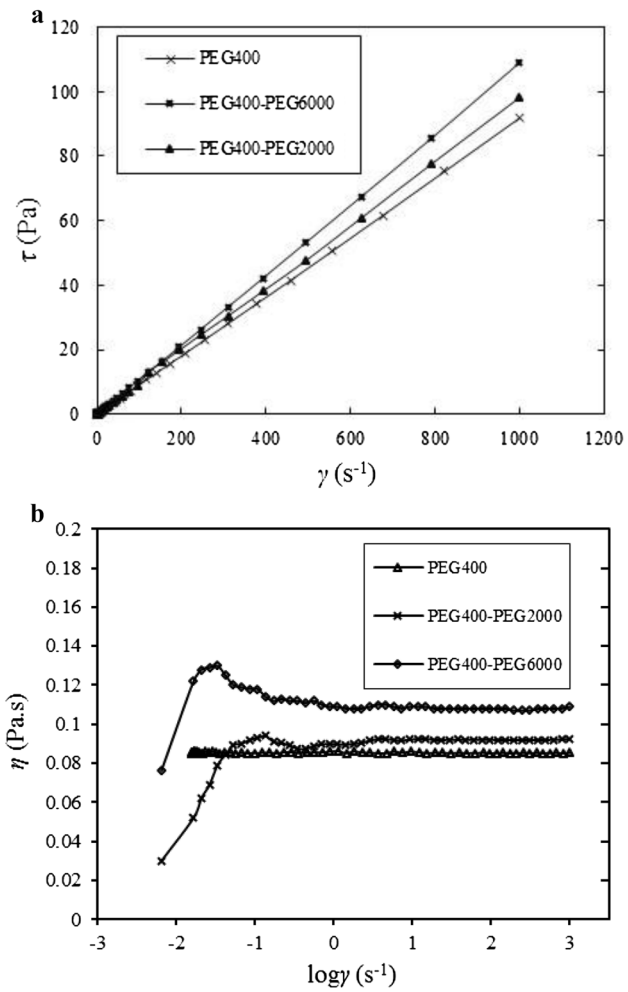

Fig. 3 **a** Shear stress versus shear rate for PEG400 and solution of PEG400-PEG2000 and PEG400-PEG6000 at $T = 298.15$ K. **b** Shear viscosity versus shear rate for PEG400 and solution of PEG400-PEG2000 and PEG400-PEG6000 at $T = 298.15$ K

3600, England). Anton Paar-Physica rheometer (MCR 300 rheometer using the two plate technique, PP 20/MR) was applied for measuring the magnetorheological properties of nanofluids. Rheological properties were measured 2–5 s after the viscometer reaching the desired shear rate. Temperature was controlled with a precision of 0.01 K. Density data were measured using a single-arm capillary pycnometer having a bulb volume of about 5 cm^3 and a capillary bore with an internal diameter of 1 mm at $T = (298.15, 308.15$ and $318.15)$ K in which the temperature was controlled with a precision of 0.1 K by a temperature controller (Julabo, MD-18 V, Germany). The uncertainty for density measurements was found to be 0.0001 g cm^{-3}.

Results and discussion

Experimental results

The bulk Fe_2O_3 and γ-Fe_2O_3 nanoparticles have been dispersed in PEG400 to prepare the homogeneous colloidal solutions with Fe_2O_3 mole fractions (x_1) of 0.0004 and 0.0008, respectively. UV–Vis spectra have been recorded for these solutions with passage of time to study the stability of colloidal solutions. The suspensions have been kept in the quartz cell without stirring throughout the recording of spectra. The recorded UV–Vis absorption spectra are presented in Fig. 1a, b. The TEM image of γ-Fe_2O_3 nanoparticles taken by producer was also shown in

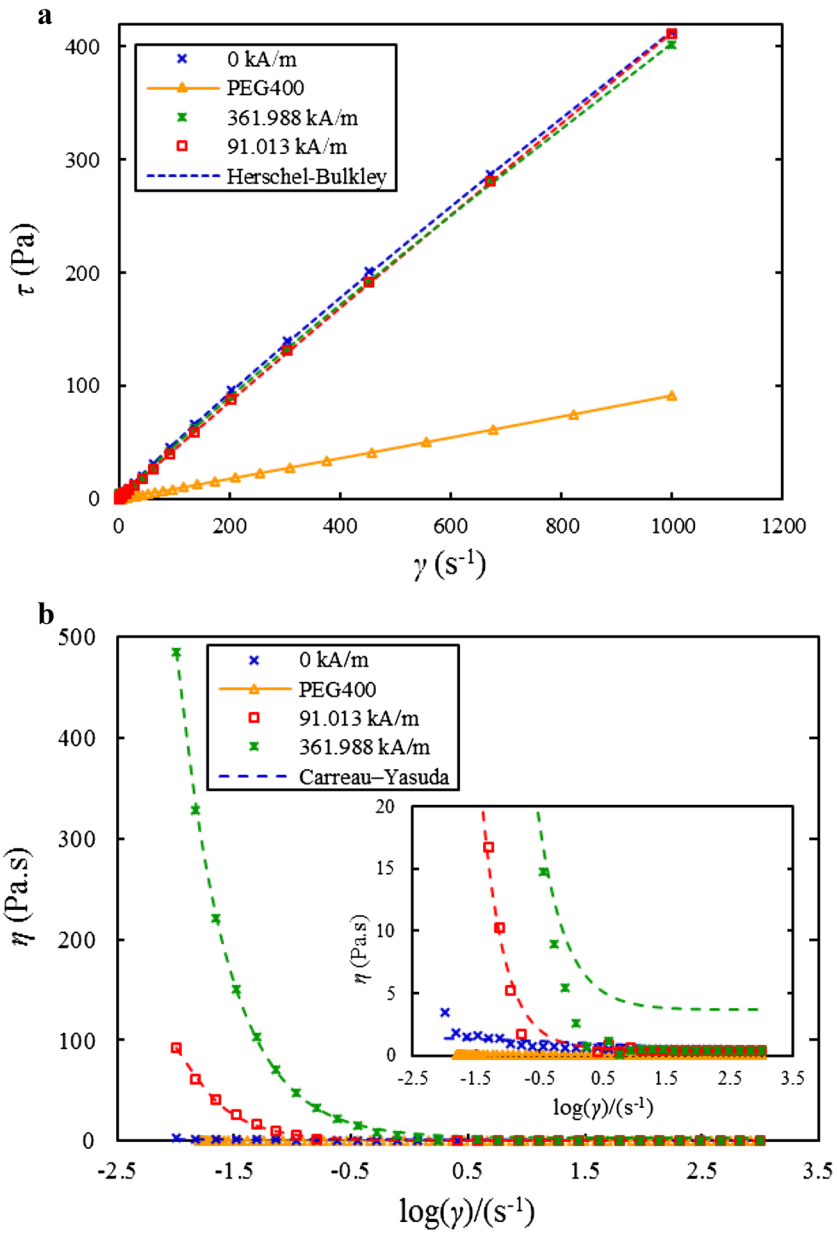

Fig. 4 **a** Shear stress versus shear rate for nanofluid of γ-Fe_2O_3-PEG400 at $\varphi_1 = 5\%$, different magnetic field and 298.15 K. **b** Shear viscosity versus shear rate for nanofluid of γ-Fe_2O_3-PEG400 at $\varphi_1 = 5\%$, different magnetic field and 298.15 K

Fig. 1b. Stability of γ-Fe_2O_3-PEG400-PEG2000 and γ-Fe_2O_3-PEG400-PEG6000 nanofluids has also been investigated by recording the UV–Vis spectra with passage of time; the mole fractions of γ-Fe_2O_3 nanoparticles (x_1) in these fluids are, respectively, 0.0006 and 0.0009. The UV–Vis absorption spectra are recorded in Fig. 1c, d. Analysis of the spectra recorded in Fig. 1a, b specify the blue shift for maximum wavelength of γ-Fe_2O_3 nanoparticles. Quantum effects like band gap enhancement with particle size decreasing are usually main reason for the blue shift of maximum absorption wavelength for particles less than about 80 Å in diameter [22, 23]. Therefore, the particle size distributions for nanofluids of γ-Fe_2O_3-PEG400 and γ-Fe_2O_3-PEG400-PEG6000 have been measured in this work. The determined mean particle sizes are, respectively, 669.0 and 672.0 nm for nanofluids of γ-Fe_2O_3-PEG400 and γ-Fe_2O_3-PEG400-PEG6000. The particle size distributions for these nanofluids are also shown in Fig. 2. The obtained particle sizes for γ-Fe_2O_3 nanoparticles in nanofluids of γ-Fe_2O_3-PEG400 and γ-Fe_2O_3-PEG400-PEG6000 are much larger than 80 Å; thereby, the blue shift of maximum absorption wavelength of UV–Vis cannot be due to the quantum effects. As we know, the optical properties of nanostructures depend on their shapes, sizes and the surrounding environment [24–26]. In this work, the preparation conditions are same for bulk-Fe_2O_3–PEG400 fluid and γ-Fe_2O_3-PEG400 nanofluid; the two main differences are the particle size of Fe_2O_3 in these fluids and interaction of

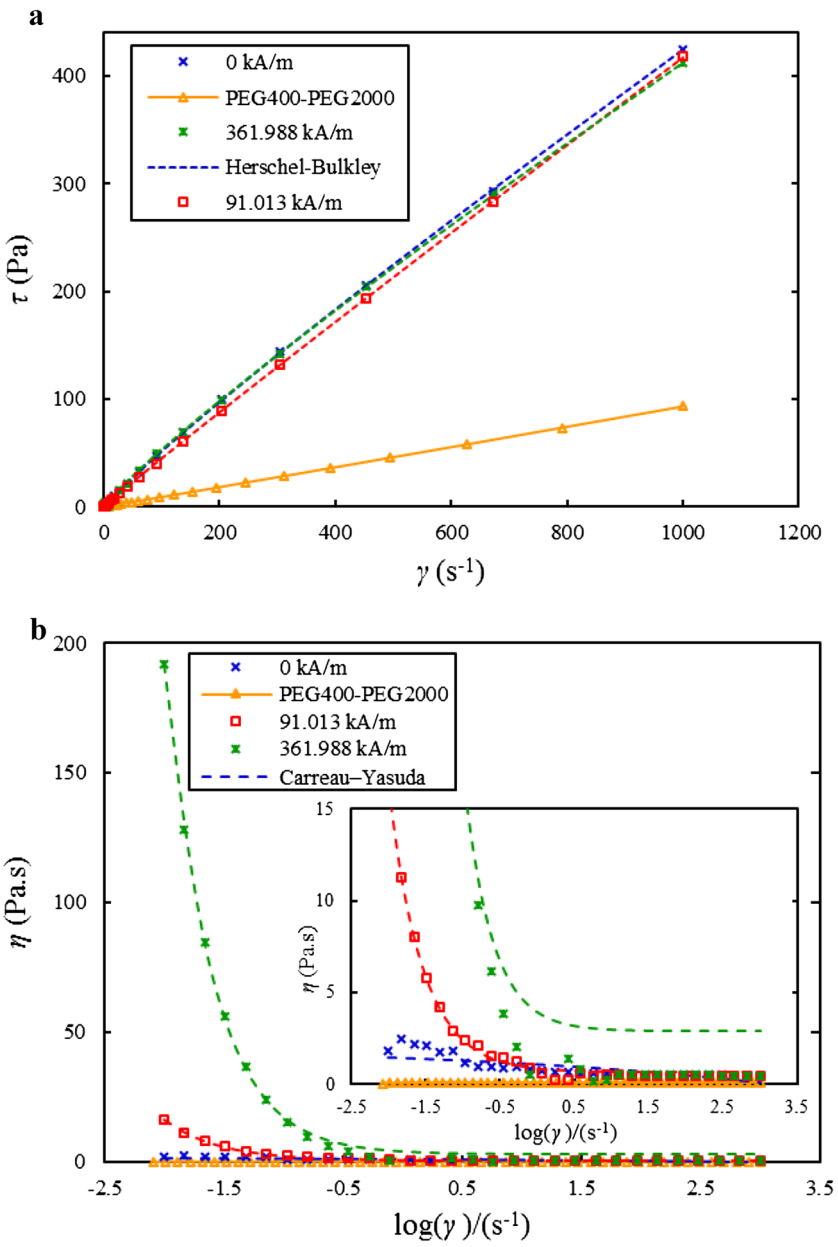

Fig. 5 **a** Shear stress versus shear rate for nanofluid of γ-Fe_2O_3-PEG400-PEG2000 at $\varphi_1 = 5\%$, different magnetic field and 298.15 K. **b** Shear viscosity versus shear rate for nanofluid of γ-Fe_2O_3-PEG400-PEG2000 at $\varphi_1 = 5\%$, different magnetic field and 298.15 K

PEG with the surface of γ-Fe_2O_3 nanoparticles which can be higher than the surface of bulk-Fe_2O_3. Therefore, the difference in particle size of Fe_2O_3 and also interaction of PEG with the surface of γ-Fe_2O_3 nanoparticles in nanofluid compared to bulk-Fe_2O_3–PEG400 fluid may be the main reasons for the blue shift observed in this work. In addition, the observed large particle sizes for studied nanoparticles are probably because of the polymer chains over nanoparticles and also aggregation forms of nanoparticles. Figure 1c, d shows that two maximum wavelengths of bulk Fe_2O_3 observed in Fig. 1a were overlapped with adding the PEG2000 and also PEG6000 to the nanofluid of γ-Fe_2O_3-PEG400. Figure 1b–d also reveals that the stability for nanofluids of γ-Fe_2O_3-PEG400, γ-Fe_2O_3-PEG400-PEG2000 and γ-Fe_2O_3-PEG400-PEG6000 is good at least for 25 days. The zeta potential values were also measured to confirm the stability of γ-Fe_2O_3-PEG400, γ-Fe_2O_3-PEG400-PEG2000 and γ-Fe_2O_3-PEG400-PEG6000 fluids. The obtained zeta potential value for all three suspensions was 200 mV. We know that a high positive or high negative value of zeta potential (> 30 mV or < -30 mV) proves the stable suspensions [25]. Therefore, in our work, the stability of the studied γ-Fe_2O_3 nanofluids is good. This can be due to the existance of an interaction between the polymer chains and the nanoparticles and also viscose environment provided by the polymer.

The rheological properties of ferrofluids using an external magnetic field have been measured to reveal the effects of γ-Fe_2O_3 nanoparticles on flow behavior of PEG400, PEG400-PEG2000 and PEG400-PEG6000

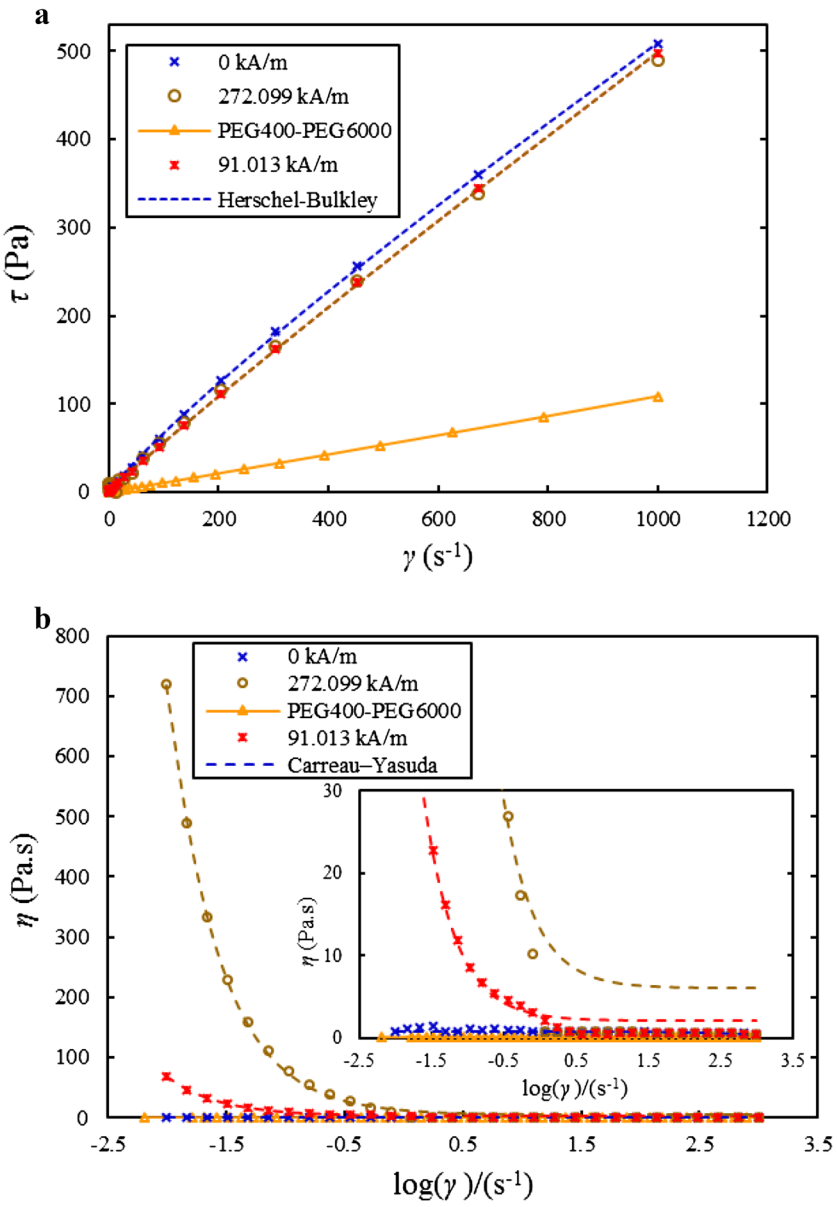

Fig. 6 **a** Shear stress versus shear rate for nanofluid of γ-Fe_2O_3-PEG400-PEG6000 at $\varphi_1 = 5\%$, different magnetic fields and 298.15 K. **b** Shear viscosity versus shear rate for nanofluid of γ-Fe_2O_3-PEG400-PEG6000 at $\varphi_1 = 5\%$, different magnetic field and 298.15 K

solutions. Therefore, we prepared the nanofluids of γ-Fe_2O_3-PEG400, γ-Fe_2O_3-PEG400-PEG2000 and γ-Fe_2O_3-PEG400-PEG6000 at two volume fractions of γ-Fe_2O_3 ($\varphi_1 = 1.5$ and 5%). These volume fractions correspond to γ-Fe_2O_3 mole fraction (x_1) of ($x_1 = 0.1512$ and 0.3819) and PEG400 mole fractions (x_2) of ($x_2 = 0.8478$ and 0.6175 for γ-Fe_2O_3-PEG400-PEG2000 nanofluid, and $x_2 = 0.8481$ and 0.6178 for γ-Fe_2O_3-PEG400-PEG6000 nanofluid). The variations of shear stress and viscosity with shear rate at different magnetic fields were measured for investigated colloidal solutions at 298.15 K. The obtained results were shown in Fig. 3 for PEG400, PEG400-PEG2000 and PEG400-PEG6000 solutions and in Figs. 4, 5 and 6 for nanofluids of γ-Fe_2O_3-PEG400, γ-Fe_2O_3-PEG400-PEG2000 and γ-Fe_2O_3-PEG400-PEG6000 at $\varphi_1 = 5\%$; and in Figs. S1–S3 as supplementary material for γ-Fe_2O_3-PEG400, γ-Fe_2O_3-PEG400-PEG2000 and γ-Fe_2O_3-PEG400-PEG6000 at $\varphi_1 = 1.5\%$. To see the variety of viscosity with shear rate increasing in a better manner, the viscosity data changes in the short range have also been illustrated inside Fig. 4b and 6b. Figure 3 indicates that the base fluid of PEG400 exhibits a Newtonian flow behavior with viscosity values of approximately 85–91.8 (mPa s) in the shear rate of 0.01–1000 s^{-1} at 298.15 K which is compatible with our previous work [17]. PEG400-PEG2000 and PEG400-PEG6000 solutions exhibit the shear thickening behavior with initial rise on shear rate; this can be due to form of some structures between PEG400 and PEG2000 or PEG6000 at very low values of shear rate. Figures 3, 4, 5 and 6 and also S1-S3 show that Newtonian flow of PEG400 and shear thickening behaviors of PEG400-PEG2000 and PEG400-PEG6000 solutions were changed to a pseudoplastic (or shear-thinning) behavior for all the suspensions investigated (γ-Fe_2O_3-PEG400, γ-Fe_2O_3-PEG400-PEG2000 and γ-Fe_2O_3-PEG400-PEG6000). This revealed that the resistance to flow was reduced by using the small forces, and the aggregations of γ-Fe_2O_3 nanoparticles or network flocs formed between PEG and γ-Fe_2O_3 were broken into the smaller flow units with shear rate increasing. In addition, large values for viscosity and shear stress have been observed at higher magnetic fields which can be due to form of chain-like structure of iron oxide. The results obtained from this work are also consistent with those we observed in our previous work for Fe_3O_4 nanoparticles coated with oleic acid—PEG nanofluid [17].

The experimental density (d) values for nanofluids of γ-Fe_2O_3-PEG400, γ-Fe_2O_3-PEG400-PEG2000 and γ-Fe_2O_3-PEG400-PEG6000 have also been measured at $T = (298.15, 308.15$ and $318.15)$ K. The obtained results are collected in Tables 1 and 2. The excess molar volume, V_m^E values have been calculated by Eq. (1) for characterizing the nonideal behavior of the investigated colloidal solutions because of the interparticle interactions.

$$V_m^E = \sum_{i=1}^{3} x_i M_i \left[\frac{1}{d} - \frac{1}{d_i}\right] \quad (1)$$

Table 1 Density (d) and excess molar volume (V_m^E), for nanofluid of γ-Fe_2O_3-PEG400 at different temperatures

$100 \times x_1^a$	$100 \times \varphi_1^b$	$\frac{d}{(\mathrm{kg\ m^{-3}})}$	$\frac{10^6 \times V_m^E}{(\mathrm{m^3\ mol^{-1}})}$
$T = 298.15$ K			
0	0	1122.6	
0.02	0.001	1116.7	1.897
0.04	0.003	1116.9	1.852
0.08	0.007	1117.1	1.840
0.13	0.011	1117.5	1.762
0.20	0.017	1117.9	1.712
0.78	0.067	1120	1.687
1.14	0.098	1120.9	1.805
2.14	0.187	1123.3	2.172
2.85	0.25	1126.7	1.905
3.62	0.32	1132.5	0.994
$T = 308.15$ K			
0	0	1114.4	
0.02	0.001	1109.8	1.503
0.04	0.003	1109.9	1.490
0.08	0.007	1109.9	1.543
0.13	0.011	1110.3	1.464
0.20	0.017	1111.0	1.316
0.78	0.066	1113.2	1.258
1.14	0.098	1114.0	1.409
2.14	0.186	1116.0	1.906
2.85	0.248	1119.6	1.571
3.62	0.318	1125.4	0.647
$T = 318.15$ K			
0	0	1106.2	
0.02	0.001	1102.9	1.107
0.04	0.003	1103	1.094
0.08	0.007	1103.1	1.115
0.13	0.011	1103.3	1.10
0.20	0.017	1103.7	1.048
0.78	0.066	1105.9	0.988
1.14	0.097	1106.7	1.140
2.14	0.184	1109.5	1.385
2.85	0.246	1113.3	0.982
3.62	0.315	1120.3	-0.325

Uncertainties for mole fraction, temperature and density are 0.0001, 0.1 K and 0.0001 g cm^{-3}, respectively

[a] x_1 is mole fraction of γ-Fe_2O_3 nanoparticles

[b] φ_1 is volume fraction of γ-Fe_2O_3 nanoparticles

Table 2 Density (d) and excess molar volume (V_m^E), for nanofluid of γ-Fe_2O_3-PEG400-PEG2000 and γ-Fe_2O_3-PEG400-PEG6000 at different temperatures

γ-Fe_2O_3-PEG400-PEG2000					γ-Fe_2O_3-PEG400-PEG6000				
$100 \times x_1^a$	$100 \times \varphi_1^b$	x_2^c	d (kg m^{-3})	$\frac{10^6 \times V_m^E}{(m^3\ mol^{-1})}$	$100 \times x_1^a$	$100 \times \varphi_1^b$	x_2^c	d (kg m^{-3})	$\frac{10^6 \times V_m^E}{(m^3\ mol^{-1})}$
$T = 298.15$ K									
0	0	0.9993	1116.4		0	0	0.9998	1116.8	
0.02	0.001	0.9991	1115.5	2.288	0.02	0.001	0.9996	1116.8	1.870
0.04	0.003	0.999	1115.5	2.308	0.04	0.003	0.9994	1116.9	1.858
0.08	0.007	0.9985	1116.1	2.167	0.08	0.007	0.9989	1117.0	1.878
0.13	0.011	0.998	1116.3	2.153	0.13	0.011	0.9985	1117.4	1.800
0.2	0.017	0.9973	1117.8	1.749	0.20	0.017	0.9978	1118.0	1.685
0.39	0.033	0.9955	1118.8	1.637	0.39	0.033	0.9959	1119.8	1.318
1.14	0.099	0.9879	1122.4	1.338	1.15	0.099	0.9883	1123.1	1.117
2.15	0.187	0.9778	1124.2	1.896	2.15	0.187	0.9783	1124.7	1.740
2.86	0.25	0.9708	1127.6	1.630	2.86	0.25	0.9712	1127.7	1.600
3.63	0.32	0.9631	1133.2	0.782	3.63	0.32	0.9635	1133.3	0.752
$T = 308.15$ K									
0	0	0.9993	1109.6		0	0	0.9998	1109.1	
0.02	0.001	0.9991	1109.7	1.540	0.02	0.001	0.9996	1109.9	1.475
0.04	0.003	0.999	1109.7	1.559	0.04	0.003	0.9994	1109.9	1.495
0.08	0.007	0.9985	1110.2	1.450	0.08	0.007	0.9989	1110.1	1.484
0.13	0.011	0.998	1110.5	1.403	0.13	0.011	0.9985	1110.7	1.340
0.2	0.017	0.9973	1111	1.319	0.20	0.017	0.9978	1111.4	1.192
0.39	0.033	0.9955	1111.9	1.238	0.39	0.033	0.9959	1112.2	1.144
1.14	0.098	0.9879	1115	1.095	1.15	0.097	0.9883	1115.4	0.964
2.15	0.186	0.9778	1116.3	1.816	2.15	0.182	0.9783	1117.1	1.544
2.86	0.248	0.9708	1119.8	1.512	2.86	0.241	0.9712	1120.0	1.399
3.63	0.318	0.9631	1125.1	0.742	3.63	0.306	0.9635	1125.6	0.457
$T = 318.15$ K									
0	0	0.9993	1101.7		0	0	0.9998	1101.2	
0.02	0.001	0.9991	1101.8	1.473	0.02	0.001	0.9996	1102.1	1.375
0.04	0.003	0.9990	1101.9	1.460	0.04	0.003	0.9994	1102.2	1.362
0.08	0.007	0.9985	1102.3	1.381	0.08	0.007	0.9989	1102.4	1.35
0.13	0.011	0.9980	1102.6	1.334	0.13	0.011	0.9985	1103.0	1.204
0.2	0.017	0.9973	1103.1	1.248	0.20	0.017	0.9978	1103.6	1.086
0.39	0.033	0.9955	1104.1	1.132	0.39	0.032	0.9959	1104.4	1.037
1.14	0.097	0.9879	1107.7	0.821	1.15	0.096	0.9883	1107.5	0.882
2.15	0.184	0.9778	1109.5	1.389	2.15	0.180	0.9783	1109.8	1.268
2.86	0.246	0.9708	1112.9	1.112	2.86	0.239	0.9712	1113.4	0.887
3.63	0.315	0.9631	1118.9	0.112	3.63	0.304	0.9635	1119.0	-0.069

Uncertainties for mole fraction, temperature and density are 0.0001, 0.1 K and 0.0001 g·cm^{-3}, respectively

[a] x_1 is mole fraction of γ-Fe_2O_3 nanoparticles

[b] φ_1 is volume fraction of γ-Fe_2O_3 nanoparticles

[c] x_2 is mole fraction of PEG400

In this equation, x is the mole fraction; M is the molar mass; subscripts 1, 2 and 3 stand for γ-Fe_2O_3 nanoparticle, PEG400 and PEG2000 or PEG6000, respectively. We used the value of 5242 (kg m^{-3}) for density of γ-Fe_2O_3 nanoparticle which is taken from literature [27]. The solutions studied are dilute and away from pure

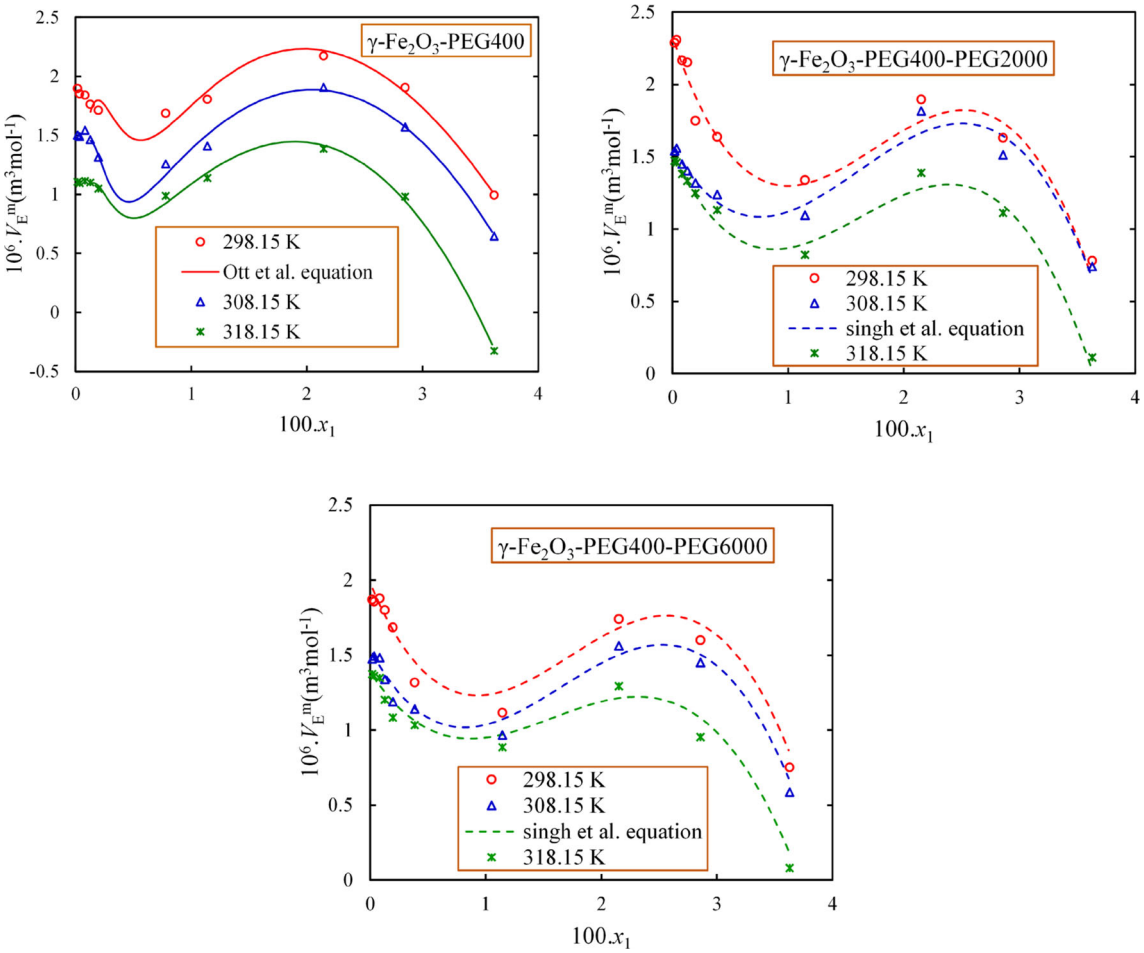

Fig. 7 Experimental and calculated excess molar volume, V_m^E, plotted against mole fraction of γ-Fe_2O_3 nanoparticle, x_1, for nanofluids of γ-Fe_2O_3-PEG400, γ-Fe_2O_3-PEG400-PEG2000 and γ-Fe_2O_3-PEG400-PEG6000 at different temperatures

nanoparticle; thereby, the calculated excess molar volumes are not very sensitive to the density data of nanoparticle at different temperatures; therefore, we can use the value of 5242 (kg m^{-3}) at three investigated temperatures. The density data for PEG 400 measured in this work are, respectively, 1122.6, 1114.4 and 1106.2 (kg m^{-3}) at $T = 298.15$, 308.15 and 318.15 K. These data are consistent with those reported in literature, (1122.30 [28] (1123.10 [29]), 1114.89 [29] and 1106.71 [29], respectively, at $T = 298.15$, 308.15 and 318.15 K). The calculated V_m^E values for the nanofluids of γ-Fe_2O_3-PEG400, γ-Fe_2O_3-PEG400-PEG2000 and γ-Fe_2O_3-PEG400-PEG6000 have been tabulated in Tables 1 and 2 and also shown in Fig. 7. As can been seen from these Tables and Fig. 7, V_m^E values for nanofluids are positive and decrease with temperature increasing. The van der Waals-type interactions which are categorized as dispersion forces can be deduced from the positive values of excess molar volume. Decreasing in interactions with rise on temperature is the main reason for decreasing of excess molar volume with temperature enhancement [30, 31]. Therefore, we can conclude that the van der Waals-type interactions are dominant in the studied nanofluids which decrease with temperature increasing. In our previous work, we also observed that the van der Waals-type interactions were dominant in ferrofluid of Fe_3O_4-PEG400 which were changed to the attractive interaction in nanofluid of Fe_3O_4-PEG400-oleic acid [17].

Modeling the experimental results

Various empirical models such as Bingham plastic and Herschel–Bulkley [18] are often used to determine the shear rate dependency of shear stress; therefore, in our work these models are applied to calculate the yield stress (critical level of stress) as follows:

$$\text{Bingham plastic model} : \tau = \tau_y + \eta\gamma \quad (2)$$

$$\text{Herschel}-\text{Bulkley model} : \tau = \tau_y + K_{HB}(\gamma)^n, \quad (3)$$

where τ_y is the yield-stress parameter; η is the suspension viscosity; K_{HB} and n are the structure-dependent

Table 3 Parameters of Bingham plastic model, Eq. (2), and Herschel–Bulkley model, Eq. (3), along with viscosity at high shear rate, η_∞, for γ-Fe_2O_3-PEG nanofluids at different magnetic field

Bingham plastic model				η_∞ (Pa.s)	Herschel–Bulkley model			
φ_1%	τ_y (Pa)	η	R^2		τ_y (Pa)	K_{HB}	n	R^2
Fe_2O_3-PEG400 at $T = 0$ kA m^{-1}								
1.5	0.34528	0.16087	0.99991	0.34528	0.25494	0.15471	1.00607	0.99999
5	2.02229	0.42197	0.99815	2.02229	0.27798	0.71985	0.91978	0.99841
Fe_2O_3-PEG400 at $T = 91.013$ kA m^{-1}								
5	0.5427	0.41593	0.99961	0.5427	0.2751	0.50063	0.97199	0.99982
Fe_2O_3-PEG400 at $T = 181.744$ kA m^{-1}								
1.5	0.76438	0.1666	0.99971	0.76438	0.26043	0.18975	0.98128	0.99992
Fe_2O_3-PEG400 at $T = 361.988$ kA m^{-1}								
5	3.68246	0.40625	0.99883	3.68246	0.2889	0.6599	0.92834	0.99874
Fe_2O_3-PEG400-PEG2000 at $T = 0$ kA m^{-1}								
1.5	1.38534	0.29937	0.99863	1.38534	0.27179	0.51347	0.91878	0.99837
5	2.13110	0.43253	0.99812	2.1311	0.27974	0.74878	0.91758	0.99832
Fe_2O_3-PEG400-PEG2000 at $T = 91.013$ kA m^{-1}								
5	0.66837	0.42052	0.99982	0.66837	0.2770	0.51284	0.97002	0.99979
Fe_2O_3-PEG400-PEG2000 at $T = 361.988$ kA m^{-1}								
1.5	3.06162	0.27395	0.99696	3.06162	0.27309	0.34232	0.96868	0.99977
5	2.89571	0.42321	0.99714	2.89571	0.28342	0.86766	0.89228	0.99706
Fe_2O_3-PEG400-PEG6000 at $T = 0$ kA m^{-1}								
1.5	2.65872	0.35622	0.99567	2.65872	0.27625	0.80425	0.87766	0.99614
5	3.60548	0.52602	0.99593	3.60548	0.28860	1.17794	0.87886	0.99622
Fe_2O_3-PEG400-PEG6000 at $T = 91.013$ kA m^{-1}								
5	2.16002	0.50516	0.99922	2.16002	0.28823	0.72802	0.94532	0.99928
Fe_2O_3-PEG400-PEG6000 at $T = 272.099$ kA m^{-1}								
1.5	1.41867	0.3361	0.99927	1.41867	0.27494	0.49009	0.94348	0.99923
5	6.09453	0.49362	0.99723	6.09453	1.01166	0.84459	0.92086	0.99846
Fe_2O_3-PEG400-PEG6000 at $T = 361.988$ kA m^{-1}								
1.5	2.21593	0.32215	0.99915	2.21593	0.28035	0.45607	0.94857	0.99937

adjustable parameters. The determined shear stress data were correlated to Eqs. (2) and (3) and the obtained results were collected in Table 3. The dashed lines in Figs. 4a and 6a and S1a–S3a illustrate the performance of Herschel–Bulkley model in fitting the shear stress values. Table 3 shows that the yield stress or critical level of stress obtained by Herschel–Bulkley model is enhanced with rise of concentration and magnetic field.

The Carreau–Yasuda model [19] as following equation is applied for correlating the viscosity values of investigated nanofluids at each concentration and magnetic field:

$$\eta = \eta_\infty + (\eta_0 - \eta_\infty)[1 + (\lambda\gamma)^a]^{\left(\frac{n-1}{a}\right)} \tag{4}$$

η_0, and η_∞ are, respectively, the viscosity of colloidal solutions at very low and high shear rates. λ, a and n are the parameters of this model. The obtained results are given in Table 4 and illustrated in Figs. 4b and 6b and S1b–S3b. As can be seen from these figures and table the performance of the Carreau–Yasuda model in fitting the viscosity values of considered nanofluids is good especially at low values of shear rate.

The excess molar volumes for nanofluid of γ-Fe_2O_3-PEG400 were correlated with Ott et al. [20] equation and V_m^E values for nanofluids of γ-Fe_2O_3-PEG400-PEG2000 and γ-Fe_2O_3-PEG400-PEG6000 were fitted with Singh et al. [21] equation. The Ott et al. [20] and Singh et al. [21] models are, respectively, shown in Eqs. (5) and (6):

$$V_m^E = x_1(1-x_1)\left[\exp(-\gamma x_1)\sum_{I=0}^{1} B_I(1-2x_1)^I + (1-\exp(-\gamma x_1))\sum_{I=0}^{3} C_I(1-2x_1)^I\right], \tag{5}$$

$$V_{m123}^E = V_{m12}^E + V_{m13}^E + V_{m23}^E + x_1x_2x_3\left[A_{123} + B_{123}x_1(x_2-x_3) + C_{123}x_1^2(x_2-x_3)^2\right], \tag{6}$$

where γ, B_I and C_I represent the adjustable parameters of Ott et al. equation. V_{m12}^E, V_{m13}^E, V_{m23}^E, A_{123}, B_{123} and C_{123}

Table 4 Parameters of Carreau–Yasuda model along with standard deviation, σ, obtained from fitting the viscosity values of γ-Fe_2O_3-PEG nanofluids

φ_1%	λ	a	n	σ (Pa.s)
Fe_2O_3-PEG400 at $T = 0$ kA m^{-1}				
1.5	51.32	1.014	0.1194	0.224
5	756.2	0.03926	1.176	0.385
Fe_2O_3-PEG400 at $T = 91.013$ kA m^{-1}				
5	93.86	16.65	− 0.2173	1.632
Fe_2O_3-PEG400 at $T = 181.744$ kA m^{-1}				
1.5	98.42	32.2	− 0.07055	0.869
Fe_2O_3-PEG400 at $T = 361.988$ kA m^{-1}				
5	99.8	61.41	− 0.01415	3.213
Fe_2O_3-PEG400-PEG2000 at $T = 0$ kA m^{-1}				
1.5	92.44	0.1502	1.048	0.090
5	287.1	0.06558	1.152	0.385
Fe_2O_3-PEG400-PEG2000 at $T = 91.013$ kA m^{-1}				
5	104.4	61.17	0.05158	0.239
Fe_2O_3-PEG400-PEG2000 at $T = 361.988$ kA m^{-1}				
1.5	101.4	49.11	0.1132	2.132
5	96.63	25.39	− 0.1435	2.403
Fe_2O_3-PEG400-PEG6000 at $T = 0$ kA m^{-1}				
1.5	53.65	8.357	− 729.6	1.924
5	0.01934	1.917	1.021	0.222
Fe_2O_3-PEG400-PEG6000 at $T = 91.013$ kA m^{-1}				
5	102.4	61.05	0.01517	1.248
Fe_2O_3-PEG400-PEG6000 at $T = 272.099$ kA m^{-1}				
1.5	122.3	57.75	0.2281	1.021
5	98.33	61.47	0.0002578	5.651
Fe_2O_3-PEG400-PEG6000 at $T = 361.988$ kA m^{-1}				
1.5	97.6	46.47	− 0.07463	1.956

[a] $\sigma = \sqrt{\frac{\sum_{i=1}^{N}(\eta_i^{exp}-\eta_i^{cal})^2}{N}}$ in which N is the total number of data

Table 5 Parameters of Ott et al. (Eq. (5)) along with standard deviations (σ) for nanofluid of γ-Fe_2O_3-PEG400 at different temperatures

γ	B_0	B_1	C_0	C_1	C_2	σ
$T = 298.15$ K						
672.594	1569.019	1249.637	3701.279	− 10330.341	6868.277	σ ($10^6 \times V_m^E$) = 0.073
						σ (d/kg m^{-3}) = 0.231
$T = 308.15$ K						
934.505	1891.648	1471.770	− 6229.640	10927.529	− 4518.774	σ ($10^6 \times V_m^E$) = 0.052
						σ (d/kg m^{-3}) = 0.164
$T = 318.15$ K						
789.895	1054.548	1047.991	− 15425.645	30216.355	− 14657.683	σ ($10^6 \times V_m^E$) = 0.097
						σ (d/kg m^{-3}) = 0.300

are the fitting coefficients of Singh et al. equation. The evaluated parameters of Ott et al. and Singh et al. equations along with standard deviations are given in Tables 5 and 6, respectively. The fitting quality of these models is also shown in Fig. 7. From this figure and Tables 5 and 6 one can conclude that the performance of the aforementioned models is good in fitting the excess molar volumes of the investigated nanofluids.

Table 6 Parameters of Singh et al. (Eq. (6)) along with standard deviations (σ) for nanofluid of γ-Fe_2O_3-PEG400 + PEG2000 and γ-Fe_2O_3-PEG400 + PEG6000 at different temperatures

V^E_{m12}	V^E_{m13}	V^E_{m23}	$10^{-5} \times A_{123}$	$10^{-7} \times B_{123}$	$10^{-8} \times C_{123}$	σ
γ-Fe_2O_3-PEG400-PEG2000						
$T = 298.15$ K						
0.7792	0.6819	0.8702	− 3.449	2.451	− 4.753	$\sigma\ (10^6 \times V^E_m) = 0.09$
						$\sigma\ (d/\mathrm{kg\ m^{-3}}) = 0.283$
$T = 308.15$ K						
0.7792	0.4828	0.8702	− 2.085	1.825	− 3.824	$\sigma\ (10^6 \times V^E_m) = 0.073$
						$\sigma\ (d/\mathrm{kg\ m^{-3}}) = 0.230$
$T = 318.15$ K						
0.7792	0.2621	0.8702	− 2.49	1.964	− 4.088	$\sigma\ (10^6 \times V^E_m) = 0.056$
						$\sigma\ (d/\mathrm{kg\ m^{-3}}) = 0.173$
γ-Fe_2O_3-PEG400-PEG6000						
$T = 298.15$ K						
0.6622	0.5892	0.7285	− 9.291	6.925	− 13.53	$\sigma\ (10^6 \times V^E_m) = 0.065$
						$\sigma\ (d/\mathrm{kg\ m^{-3}}) = 0.204$
$T = 308.15$ K						
0.6622	0.473	0.7285	− 7.242	5.950	− 12.12	$\sigma\ (10^6 \times V^E_m) = 0.049$
						$\sigma\ (d/\mathrm{kg\ m^{-3}}) = 0.152$
$T = 318.15$ K						
0.6622	0.4329	0.7285	− 5.949	4.779	− 10.22	$\sigma\ (10^6 \times V^E_m) = 0.057$
						$\sigma\ (d/\mathrm{kg\ m^{-3}}) = 0.175$

Conclusions

The homogeneous and one-phase solutions of polyethylene glycols, PEGs, with molar masses of 2000 and 6000 (g mol^{-1}) in PEG with molar mass of 400 (g mol^{-1}) were prepared. Rheological properties and density values for these solutions have been measured at different temperatures. Nanoparticles of γ-Fe_2O_3 were added to these solutions and dispersed by an ultrasonic bath to make homogeneous nanofluids. The UV–Vis spectroscopy, zeta potential and dynamic light scattering have been used to specify the stability and particle size distribution of the colloidal solutions studied. Result analysis of these methods revealed that the investigated nanofluids are reversibly stable for a long time. This indicates that the low toxicity and water-soluble base fluids considered in this work can be convenient for making the stable ferrofluids with others magnetic nanoparticles by two-step method. The main reasons for the blue shift of maximum absorption wavelength of UV–Vis spectra can be due to the difference in particle size of Fe_2O_3 in nanofluid compared to bulk-Fe_2O_3–PEG400 fluid, and also the interaction of PEG with the surface of γ-Fe_2O_3 nanoparticles can be higher than the surface of bulk-Fe_2O_3. Rheological behaviors of γ-Fe_2O_3 nanoparticles dispersed in PEGs have been investigated in volumetric solid concentrations of $\varphi_1 = 1.5$ and 5% and shear rates ($\gamma = 0.01$–$1000\ s^{-1}$) at different magnetic fields and $T = 298.15$ K. Newtonian flow behavior of PEG400 and shear thickening behaviors of solutions (PEG400-PEG2000 and PEG400-PEG6000) were changed to a pseudoplastic (or shear-thinning) behavior for all the suspensions investigated (γ-Fe_2O_3-PEG400, γ-Fe_2O_3-PEG400-PEG2000 and γ-Fe_2O_3-PEG400-PEG6000). The trend of excess molar volumes of the nanofluids with concentration and temperature indicates that the significant interactions observed in the studied colloidal solutions are van der Waals-type interactions. Bingham plastic, Herschel–Bulkley and Carreau–Yasuda models have successfully been applied for modeling the magnetorheological properties of nanofluids. The excess molar volume values were adequately fitted to the Ott et al. and Singh et al. equations.

Acknowledgement We are grateful to Iranian Nanotechnology Initiative Council for the financial support of this research.

Compliance with ethical standards

Conflict of interest The authors have no conflict of interest.

References

1. Viota JL, Gozález-Caballero F, Durán JDG, Delgado AV (2007) Study of the colloidal stability of concentrated bimodal magnetic fluids. J Colloid Interface Sci 309:135–139
2. Alexious C, Arnold W, Hulin P, Klein RJ, Renz H, Parak FG, Bergemann C (2001) Magnetic mitoxantrone nanoparticle detection by histology, X-ray and MRI after magnetic tumor targeting. J Magn Magn Mater 225:187–193
3. Jordan A, Scholz R, Wust P, Fähling H, Felix R (1999) Magnetic fluid hyperthermia (MFH): cancer treatment with AC magnetic field induced excitation of biocompatible superparamagnetic nanoparticles. J Magn Magn Mater 201:413–419
4. Mykhaylyk O, Cherchenko A, Ilkin A, Dudchenko N, Ruditsa V (2001) Glial brain tumor targeting of magnetite nanoparticles in rats. J Magn Magn Mater 225:241–247
5. Nalam PC, Clasohm JN, Mashaghi A, Spencer ND (2009) Macrotribological studies of poly(L-lysine)-graft-poly(ethylene glycol) in aqueous glycerol mixtures. Tribol Lett 37:541–552
6. Hosseini M, Ghader S (2010) A model for temperature and particle volume fraction effect on nanofluid viscosity. J Mol Liq 153:139–145
7. Wei Ch, Nan Zh, Wang X, Tan Zh (2010) Investigation on thermodynamic properties of a water-based hematite nanofluid. J Chem Eng Data 55:2524–2528
8. Guo Sh-Zh, Li Y, J-s Jiang, Xie H-Q (2010) Nanofluids containing γ-Fe_2O_3 nanoparticles and their heat transfer enhancements. Nanoscale Res Lett 5:1222–1227
9. Colla L, Fedele L, Scattolini M, Bobbo S (2012) Water-based Fe_2O_3 nanofluid characterization: thermal conductivity and viscosity measurements and correlation. Adv Mech Eng 2012(674947):1–8
10. Gayadhthri V, Suganthi KS, Manikandan S, Rajan KS (2014) Role of surfactants in colloidal stability and properties of α-Fe_2O_3 based nanofluids. Asian J Sci Res 320(327):1–8
11. Rajnak M, Timko M, Kopcansky P, Paulovicova K, Tothova J, Kurimsky J, Dolnik B, Cimbala R, Avdeev MV, Petrenko VI, Feoktystov A (2017) Structure and viscosity of a transformer oil-based ferrofluid under an external electric field. J Magn Magn Mater 43:99–102
12. Katiyar A, Dhar P, Nandi T, Das SK (2017) Magnetoviscoelastic characteristics of superparamagnetic oxides (Fe, Ni) based ferrofluids. J Magn Magn Mater 436:35–46
13. Felicia LJ, Vinod S, Philip J (2016) Recent advances in magnetorheology of ferrofluids (magnetic nanofluids)—a critical review. J Nanofluids 5:1–22
14. Cunha FR, Rosa AP, Dias NJ (2016) Rheology of a very dilute magnetic suspension with micro-structures of nanoparticles. J Magn Magn Mater 397:266–274
15. Alphonse P, Bleta R, Soules R (2009) Effect of PEG on rheology and stability of nanocrystalline titania hydrosols. J Colloid Interface Sci 337:81–87
16. Zhang H, Wu Q, Lin J, Chen J, Xu Z (2010) Thermal conductivity of polyethylene glycol nanofluids containing carbon coated metal nanoparticles. J Appl Phys 108:124304
17. Zafarani-Moattar MT, Majdan-Cegincara R (2013) Stability, rheological, magnetorheological and volumetric characterizations of polymer based magnetic nanofluids. Colloid Polym Sci 291:1977–1987
18. Reed JS (1995) Principles of ceramics processing. Wiley, New York USA
19. Bird RB, Armstrong RC, Hassager O (1987) Dynamics of polymer liquids, vol 1, 2nd edn. Wiley, New York
20. Ott JB, Stouffer CE, Cornett GV, Woodfield BF, Wirthlin RC, Christensen JJ, Dieters JA (1986) Excess enthalpies for (ethanol + water) at 298.15 K and pressures of 0.4, 5, 10, and 15 MPa. J Chem Thermodyn 18:1–12
21. Singh PP, Nikam RK, Sharma SP, Aggarwal S (1984) Molar excess volumes of ternary mixtures of nonelectrolytes. Fluid Phase Equilib 18:333–334
22. Hu Z, Oskam G, Penn RL, Pesika N, Searson PC (2003) The influence of anion on the coarsening kinetics of ZnO nanoparticles. J Phys Chem B 107:3124–3130
23. Wong EM, Hoertz PG, Liang CJ, Shi BM, Meyer GJ, Searson PC (2001) Influence of organic capping ligands on the growth kinetics of ZnO nanoparticles. Langmuir 17:8362–8367
24. Mogensen K B, Kneipp K (2014). Blue shift of the silver plasmon band using controlled nanoparticle dissolution in aqueous solution. In: Proceedings of Nanotech 2014
25. Wu S, Zhu D, Li X, Li H, Lei J (2009) Thermal energy storage behavior of Al_2O_3–H_2O nanofluids. Thermochim Acta 483:73–77
26. Kumar H, Rani R (2013) Structural and optical characterization of ZnO nanoparticles synthesized by microemulsion route. ILCPA 14:26–36
27. England: Kurt J Lesker Company Ltd. 2012-01-05. Retrieved 2014-07-12
28. Muller EA, Rusmussen P (1991) Densities and excess volumes in aqueous poly(ethylene glycol) solutions. J Chem Eng Data 36(1991):214–217
29. Zafarani-Moattar MT, Tohidifar N (2008) Vapor-liquid equilibria, density, speed of sound, and viscosity for the system poly(-ethylene glycol) 400 + ethanol at different temperatures. J Chem Eng Data 53(2008):785–793
30. Mutalik V, Manjeshwar LS, Sairam M, Aminabhavi TM (2006) Thermodynamic interactions in binary mixtures of anisole with ethanol, propan-1-ol, propan-2-ol, butan-1-ol, pentan-1-ol, and 3-methylbutan-1-ol at $T = (298.15, 303.15, \text{and } 308.15)$ K. J Chem Thermodyn 38:1620–1628
31. Valtz A, Teodorescu M, Wichterle I, Richon D (2004) Liquid densities and excess molar volumes for water + diethylene glycolamine, and water, methanol, ethanol, 1-propanol + triethylene glycol binary systems at atmospheric pressure and temperatures in the range of 283.15–363.15 K. Fluid Phase Equilib 215:129–142